

## Large hysteretic magnetoresistance of silicide nanostructures

T. Kim,<sup>1</sup> B. Naser,<sup>1</sup> R. V. Chamberlin,<sup>2</sup> M. V. Schilfgaarde,<sup>3</sup> P. A. Bennett,<sup>2</sup> and J. P. Bird<sup>4</sup>

<sup>1</sup>Department of Electrical Engineering, Arizona State University, Tempe, Arizona 85287-5706, USA

<sup>2</sup>Department of Physics, Arizona State University, Tempe, Arizona 85287-1504, USA

<sup>3</sup>School of Materials, Arizona State University, Tempe, Arizona 85287-6006, USA

<sup>4</sup>Department of Electrical Engineering, University at Buffalo, Buffalo, New York 14260-1920, USA

(Received 2 May 2007; revised manuscript received 20 August 2007; published 6 November 2007)

We demonstrate a large (as much as 100%) and strongly hysteretic magnetoresistance (MR) in nominally nonferromagnetic silicide films and nanowires. This unusual MR is quenched above a few kelvins, where conventional behavior due to weak antilocalization is recovered. The dynamic characteristics of this effect are suggestive of weakly interacting, localized paramagnetic moments that form at the surface oxide of the silicide nanostructures, with dramatic consequences for transport when the system size is reduced to the nanoscale.

DOI: [10.1103/PhysRevB.76.184404](https://doi.org/10.1103/PhysRevB.76.184404)

PACS number(s): 75.47.-m, 73.63.-b, 75.70.-i, 73.20.Fz

### I. INTRODUCTION

There is much interest in exploiting the surface modification of nanostructures for the development of chemical and biological sensors. Among recent demonstrations in this area include modification of the electrical characteristics of metal-semiconductor junctions via chemical functionalization,<sup>1</sup> and the use of silicon nanowires as chemical detectors.<sup>2</sup> Surface modifications can also give rise to magnetic characteristics, a notable example of which is provided by recent work on Cu nanojunctions.<sup>3,4</sup> These have been shown to exhibit spin-polarized transport at room temperature that has been attributed to oxidation of the atomic-scale junctions, resulting in the formation of half-metallic CuO. Theoretical work has predicted the possibility of magnetism at Si surfaces due to the ordering of the unpaired spins associated with naturally occurring dangling bonds (DBs).<sup>5,6</sup> Consistent with this, Curie-Weiss behavior has been found<sup>7</sup> near the metal-insulator transition in the low-temperature magnetic susceptibility of  $\text{Ti}_{1-x}\text{Si}_x$ . Electron-spin resonance revealed the source of this magnetic moment to indeed be the DBs of the amorphous Si network. The presence of a permanent magnetic moment has also been demonstrated for alkanethiol-capped gold nanoparticles,<sup>8</sup> as well as for self-assembled alkanethiol monolayers on gold surfaces,<sup>9</sup> the origins of which have been much debated.<sup>10-14</sup> Most recently, it has been suggested that the source of this magnetism may be localized surface charges and/or spins.<sup>14</sup>

The role of surface-induced modifications can be critical to understand the properties of nanomaterials and may be probed experimentally with an external magnetic field. In typical metals, this gives rise to a small ( $\sim 1\%$ ) magnetoresistance (MR), with a contribution from quantum-mechanical weak localization (WL) at low temperatures.<sup>15</sup> In this work, however, we demonstrate a large (as much as 100%) and strongly hysteretic MR in nominally nonferromagnetic silicide films and nanowires (NWs). This anomalous MR is quenched above a few kelvins, where conventional behavior due to weak antilocalization (WAL) is recovered. The dynamic characteristics of this effect, which resembles the *butterfly* hysteresis exhibited by systems of weakly interacting molecular magnets,<sup>16-18</sup> are suggestive of weakly interacting

localized paramagnetic moments that form at the surface oxide of the silicide nanostructures. On the basis of these experimental results, we speculate that the source of these localized moments is thought to be the DBs that arise in this region, and the large MR is presumed to result from the interaction of conducting electrons with localized DB spins. Our data suggest that this interaction can have dramatic consequences for transport when the system size is reduced to the nanoscale in one or more dimensions.

### II. TRANSITION-METAL DISILICIDES: A BRIEF OVERVIEW

Transition-metal disilicides (e.g.,  $\text{TiSi}_2$ ,  $\text{NiSi}_2$ ,  $\text{CoSi}_2$ ,  $\text{WSi}_2$ , etc.) represent a vital material in modern microelectronics and their electrical, magnetic, mechanical, and thermal properties have been extensively reviewed in the past.<sup>19,20</sup> In their bulk state, these compound metals are largely nonmagnetic, even for many of the silicides that are formed from the reaction of silicon with ferromagnetic metals, such as Ni and Co. (A notable exception is provided by  $\text{FeSi}_2$ , which is known to be ferromagnetic in its metallic  $\gamma$  phase.<sup>21</sup>) Generally, the temperature-dependent variation of the resistivity (between 10 and 300 K) of these materials therefore shows behavior fairly typical of nonmagnetic metals, with dominant contributions from electron-impurity and electron-phonon scatterings.<sup>19</sup> The residual resistivity of annealed polycrystalline films is typically found to be of the order tens of  $\mu\Omega$  cm for films with thicknesses down to a few nanometers. In terms of the phenomena of interest here, there have been very few studies of quantum-interference effects in transport through silicides. One notable exception is provided by the study of Jentzsch *et al.*, who investigated the WL correction in epitaxial  $\text{NiSi}_2$  films.<sup>22</sup> They reported a positive magnetoresistance arising from WAL, indicating a strong role of spin-orbit coupling as is typical for transition metals.<sup>15</sup> There was no discussion in their work of the effects that we will report, which is likely due to the fact that their measurements were limited to higher temperatures ( $\geq 1.5$  K) than ours.

Studies of quantum transport in silicide nanostructures have also been few in numbers. Lenssen and Mantl studied

quantum transport in disordered  $\text{CoSi}_2$  wires formed by ion-beam synthesis.<sup>23</sup> They also found clear evidence of WAL due to strong spin-orbit coupling, but their measurements were also restricted to higher temperatures ( $\geq 2$  K) than we considered here. More recently, we have performed both *in situ*<sup>24</sup> and *ex situ*<sup>25</sup> measurements of the electrical properties of various silicide NWs. *In situ* measurements of epitaxial  $\text{CoSi}_2$  NWs, performed under UHV conditions, reveal the pristine nature of these structures, with resistivities as low as  $30 \mu\Omega \text{ cm}$ .<sup>24</sup> *Ex situ* measurements of  $\text{NiSi}_2$  NWs, however, suggest a much higher residual resistivity ( $\sim 800 \mu\Omega \text{ cm}$ ), which has been suggested to be associated with the effects of enhanced surface scattering from roughness caused by oxidation.<sup>25</sup>

### III. EXPERIMENTAL METHODS

The  $\text{NiSi}_2$  NWs utilized in this study were grown on  $8^\circ$ -miscut Si(111) substrates ( $10 \Omega \text{ cm}$ ) by the process of reactive epitaxy. For further details on the epitaxial growth and structural characterization of the resulting crystalline NWs, we refer the reader to Ref. 25 and references therein. To allow electrical measurement, metallic electrodes were fabricated on top of the NWs using a combination of optical and electron-beam lithography (EBL). The use of an appropriate system of alignment markers in the EBL allowed the successful contacting of individual NWs by multiple electrodes, as shown in Fig. 1(b). Prior to the deposition of the EBL-defined (Ni/Au: 50/200 Å) electrodes, regions of native oxide at the contact area were removed by exposing the sample to a 20:1 buffered-oxide etchant for 6 s prior to metal deposition.<sup>25</sup> Preliminary experimental measurements of the electrical properties of these NWs were reported in Ref. 25. The typical NW dimensions are 90 nm width and 30 nm thickness.  $\text{TiSi}_2$  films were grown by molecular-beam epitaxy on a Si(100) substrate using a cleaning recipe that provides a smooth hydrogen-terminated surface prior to epitaxy. The substrate temperature was maintained at  $400^\circ \text{C}$  during the metal deposition to allow the silicide reaction to occur. We have measured the properties of two different types of film: an uncapped 45 Å film of  $\text{TiSi}_2$  and a 7 Å film of  $\text{TiSi}_2$  that was capped with 50 Å of amorphous silicon (the film thicknesses quoted here were determined by Rutherford backscattering.) To allow electrical measurements of the films, palladium or gold contacts were evaporated onto their surface in a lithographically defined pattern and were annealed for several minutes at  $\sim 200^\circ \text{C}$  in a controlled atmosphere.

The different samples were bonded into ceramic chip carriers and their magnetoresistance was measured in an Oxford Instruments Kelvinox-300 dilution refrigerator (0.02–4.2 K). For these measurements, the chip carriers were bolted to a copper cold finger of the mixing chamber that extended to the center of the superconducting magnet. (We emphasize that the samples were situated *in vacuum* under these conditions and were *not* mounted in direct contact with the dilution-fridge mixture.) The cryostat temperature was measured with a low-magnetoresistance  $\text{RuO}_2$  chip resistor, which was mounted on the mixing chamber in a

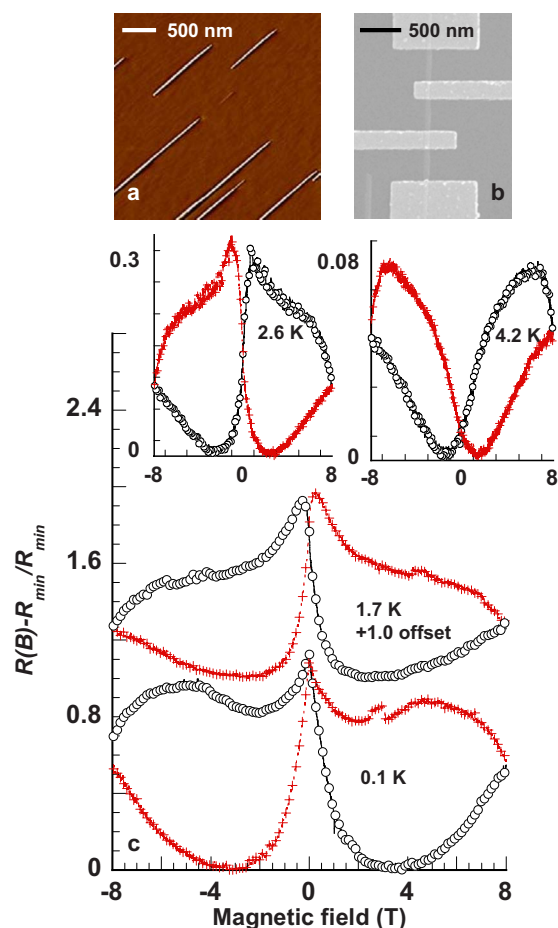


FIG. 1. (Color online) (a) Scanning AFM image of the epitaxially formed  $\text{NiSi}_2$  NWs. (b) Scanning electron micrograph showing the individually contacted  $\text{NiSi}_2$  NW whose MR characteristics are plotted in the figure. (c) MR of the  $\text{NiSi}_2$  NW at several different temperatures (indicated). Open circles were obtained while sweeping  $B$  from  $+8$  to  $-8$  T, while red crosses were obtained sweeping from  $-8$  to  $+8$  T. In all cases, the magnetic-field sweep rate was  $0.2 \text{ T/min}$ .

field-compensated region for which stray magnetic fields were limited to a few tens of milliteslas. Calibration of this thermometer against a nuclear-orientation primary thermometer indicated that it remained in good thermal contact (with proper rf shielding) with the mixing chamber to temperatures below 20 mK. The cold finger (also manufactured by Oxford Instruments) was designed to minimize eddy heating during magnetic field sweeps, so that the *maximum* temperature rise observed in this study while sweeping at base temperatures was less than 25 mK. In order to achieve a high signal-to-noise ratio ( $\sim 100$ ) in our measurements, low-frequency ( $\sim 11 \text{ Hz}$ ) lock-in detection was used in these measurements, and all signal lines were filtered at the input to the cryostat to reduce rf heating. The measurements employed a constant-current circuit, with the value of the current (typically of order a few nanoamperes) chosen to ensure a voltage drop of only a few microvolts across the sample at the lowest temperatures. Magnetic field was applied normal to the plane of the NWs and films.

## IV. EXPERIMENTAL RESULTS

An example of the hysteretic MR is shown for a  $\text{NiSi}_2$  NW in Fig. 1. Figure 1(a) is an atomic force microscopy (AFM) scan of epitaxially formed NWs on a miscut Si(111) substrate. Figure 1(b) is a scanning electron micrograph of a single NW with Ni/Au measurement leads defined by electron-beam lithography. Figure 1(c) shows the NW MR for different magnetic-field ( $B$ ) sweep directions and several temperatures ( $T$ ). We emphasize again that  $\text{NiSi}_2$  is a widely studied material and is known to be nonmagnetic in bulk.<sup>19,20</sup> Nonetheless, the data of Fig. 1(c) show a pronounced hysteresis. We have previously studied the MR of similar NWs in the temperature range of 4.2–30 K and did not find evidence for this hysteresis.<sup>25</sup> Consistent with this, the 4.2 K data in Fig. 1(c) show only a weak, but still resolvable, hysteresis. The usual<sup>22</sup> positive MR due to WAL (Refs. 15 and 26) can be clearly seen here, and its size of a few percent is consistent with expectations for disordered metals.

As temperature is lowered below 4.2 K, two pronounced effects occur in the MR. The first is a transition from a positive to a negative MR, particularly in the region near zero field. This seems to distort the usual MR due to WAL, giving rise to a variation as large as 100% at the lowest  $T$ . The negative MR grows with decreasing  $T$  and is accompanied by the appearance of pronounced hysteresis. The hysteresis implies the development of a weak internal magnetization, with a characteristic energy scale of that is only of order a few kelvins. In fact, the quantitative shape of the hysteresis is reminiscent of the butterfly form found in superparamagnetic systems such as high-spin molecules.<sup>16–18</sup> In these systems, there is only a weak interaction between the molecules, which results in behavior intermediate between paramagnetic and ferromagnetic. In contrast to such magnetic systems, however, bulk  $\text{NiSi}_2$  is nonmagnetic and the hysteresis in the NW MR is therefore a great surprise.

We have measured the low-temperature MR of several  $\text{NiSi}_2$  NWs and find that all show similar hysteretic MR, independent of their measurement configuration (two- or four probes). In Fig. 2, we show the results of MR measurements of epitaxial  $\text{TiSi}_2$  films with alloyed Pd contacts, which exhibit a hysteresis similar to that found in the  $\text{NiSi}_2$  NWs. As  $T$  is lowered below 5.1 K, we again see a transition from positive to negative MR near  $B=0$  that is accompanied by the development of the hysteresis. Although the exact form for the MR line shape is different in Figs. 1 and 2, its temperature dependence and characteristic field scales are similar. Since neither Pd nor Ti is magnetic, these results are a crucial indication that the hysteresis is not related to the bulk magnetic properties. The maximum hysteresis is smaller in Fig. 2 ( $\sim 10\%$ ) than in Fig. 1, consistent with the different sample geometries (NW vs film). While Fig. 2 shows measurements of a 7 Å film, we have also made measurements of a 45 Å film and find an even smaller hysteresis ( $\sim 1\%$ ). The suggestion therefore is that the interaction between the conduction electrons and the internal moments responsible for the hysteresis becomes more pronounced as the cross-sectional area of the conductor decreases. (We estimate this area to be  $\sim 10^{-11}$ ,  $\sim 10^{-12}$ , and  $\sim 10^{-15}$  m<sup>2</sup> for the 45 Å film, 7 Å film, and NWs, respectively).

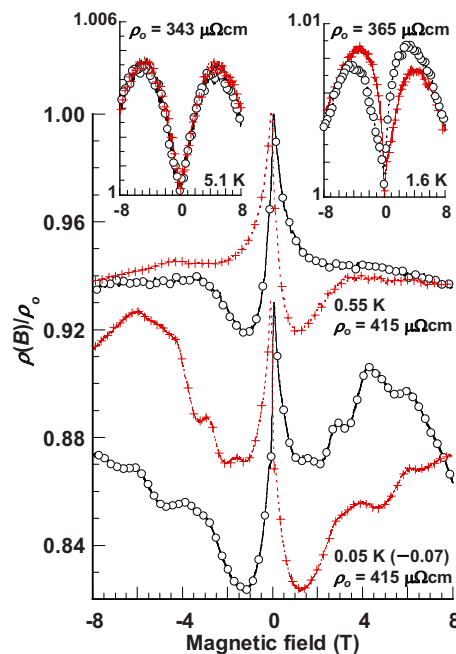


FIG. 2. (Color online) Hysteretic magnetoresistance in a  $\text{TiSi}_2$  film. MR measurements are shown at several different temperatures. Open circles were obtained while sweeping  $B$  from +8 to -8 T, while red crosses were obtained sweeping from -8 to +8 T. In all cases, the magnetic-field sweep rate was 0.1 T/min.

To characterize the internal magnetization, Fig. 3 shows the measurements of the NW of Fig. 1 for different ranges of  $B$ . The MR is reversible at low fields (1-T sweep), while hysteresis develops beginning at  $\sim 2$  T. From these results, we suggest the hysteresis curve for the internal magnetization

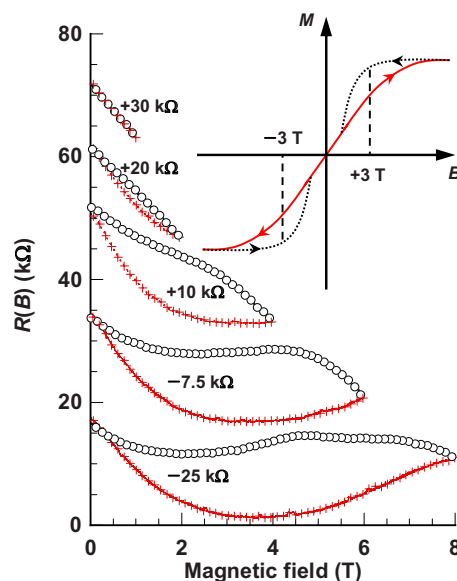


FIG. 3. (Color online) Evolution of the hysteretic MR with field-sweep range. Data are shown for the NW of Fig. 1. In all cases, the magnetic-field sweep rate was 0.2 T/min. In the inset to the figure, we show schematically the form of the hysteresis of the internal magnetization suggested by the data in the main panel.



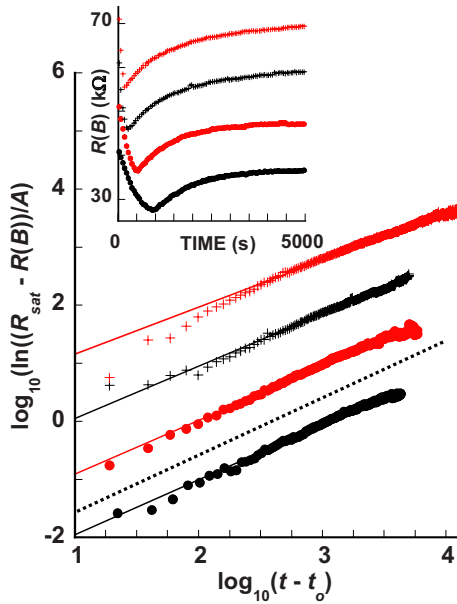


FIG. 4. (Color online) Dynamic character of the low-temperature MR. Inset: time dependence of the resistance of the NW of Fig. 1, obtained after sweeping to and then holding at a field of 2 T. Sweeps are performed at different field-sweep rates (red crosses, 0.6 T/min; black crosses, 0.4 T/min; red circles, 0.2 T/min; and black circles, 0.1 T/min) at a fixed cryostat temperature of 0.1 K. Curves are shifted by +10, +27, and +33 k $\Omega$  for sweep rates of 0.2, 0.4, and 0.6 T/min, respectively. In the main panel, the data in the inset are plotted to reveal its stretched-exponential form. Solid lines through the data are guides to the eye. Dotted line has slope of 1 and corresponds to pure exponential behavior. Curves are shifted by +1.0, +2.0, and +3.0 for sweep rates of 0.2, 0.4, and 0.6 T/min, respectively.

tion shown on the right side of Fig. 3. Such hysteresis is common in weaklyinteracting molecular magnets,<sup>16–18</sup> and has also been found for ferromagnetic alloys<sup>27–29</sup> when their magnetic dopants are dilute enough ( $\sim 10\%$ – $20\%$ ) to yield a crossover to spin-glass (SG)-like behavior. The magnitude of the MR in these alloys is very much smaller<sup>29</sup> ( $\sim 2\%$ ) than that which we observe and is possibly due to quenched amorphous structure in the bulk SG alloy. However, like our observations, the SG systems show a negative MR, with hysteresis and an asymmetric parabolic form (with respect to field reversal), which has been attributed to remnant internal magnetization.

The inset of Fig. 4 shows measurements of the time-dependent resistance of the NiSi<sub>2</sub> NW of Fig. 1, obtained by ramping  $B$  to 2 T at different rates and monitoring the resistance change as a function of time at this final field. In all curves, the resistance reaches a minimum value ( $R_{min}$ ) by the end of the sweep, after which it grows slowly, while  $B$  is fixed. We attribute this time-dependent behavior to the decay of an internal magnetization ( $M$ ) toward an equilibrium value ( $M_0$ ). A characteristic feature of SG systems is that such dynamics exhibits a *stretched* exponential form [ $\propto \exp[-(t/\tau)^\beta]$ ], in which the parameter  $\beta$  provides a measure of the intermoment interaction strength<sup>30</sup> ( $\beta=1$  for non-interacting moments, while  $\beta < 1$  for cooperative relaxation).

Assuming that this leads to a time-dependent resistance variation  $R(t) = R_{sat} - A \exp[-(t-t_0)/\tau]^\beta$ , where  $R_{sat}$  is the resistance in the long-time limit,  $A \equiv R_{sat} - R_{min}$ , and the initial field ramp ends at time  $t_0$ , we replot this data as described in Ref. 30 to reveal the stretched form in the main panel of Fig. 4. The dotted line in this figure has a slope of 1 and corresponds to a simple exponential ( $\beta=1$ ). Using the data in this figure, we obtain  $\beta=0.95$ , 0.93, 0.91, and 0.81 for sweeps rates of 0.1, 0.2, 0.4, and 0.6 T/min, respectively. While these values are closer to 1 than those typical of many SG systems ( $\beta < 0.4$ ),<sup>31</sup> they nonetheless show a statistically meaningful difference (their error is just a few percent) from  $\beta=1$  and therefore indicate some weak interaction of local moments. Indeed, the very low temperature required to quench the hysteretic MR is consistent with the idea of such a weak interaction. It is also interesting to emphasize again the similarity of our results to those obtained for weakly interacting ensembles of molecular magnets, which have been found to show similar dynamical properties to those that we report here.<sup>16</sup>

The time constant governing the quasiexponential decay of the resistance in Fig. 4 is of the order of tens of minutes (1068, 1067, 1446, 1771 s for sweep rates of 0.1, 0.2, 0.4, and 0.6 T/min, respectively). The observed increase in  $\tau$  with increasing sweep rate is opposite to what is expected from the linear response of a distribution of independent relaxation times,<sup>32</sup> indicating that the induced magnetization is a nonlinear function of external-field sweep rate. Additional support for the picture of interacting spins comes from the time scales, which are many orders of magnitude slower than the typical relaxation times of  $10^{-9}$ – $10^{-6}$  s for the internal magnetization arising from independent electron spins.<sup>33</sup>

## V. ANALYSIS OF THE EXPERIMENTAL RESULTS

### A. Excluded mechanisms for the hysteretic magnetoresistance

It is our view that a systematic and consistent interpretation of the results of Figs. 1–4 requires an interpretation in which an internal magnetization develops at low temperatures in the silicide films and NWs. A hysteretic variation of cryostat temperature during the magnetic field sweeps can be safely ruled out, since the temperature of the mixing chamber was monitored constantly during the MR measurements and showed only a small variation during magnetic field sweeps, with no correlation to the hysteresis in the MR. For the *fastest* field-sweep rate considered here (0.6 T/min), for example, the maximum temperature rise observed in experiment was 25 mK at base temperature. For such a small variation, the zero-field resistance of the films and NWs that we studied changed by no more than 5%, much smaller than the observed hysteresis in the MR.

Contamination with magnetic impurities is another possible source of the hysteresis that we believe can be reasonably ruled out. As we have mentioned, a significant concentration ( $\sim 10\%$ ) of the latter would be required to produce the observed behavior,<sup>27–29</sup> while magnetic contamination in our samples is expected to only be a few ppm. In spite of this statement, it would clearly be desirable in the future to make

direct measurements of the NW magnetization. We have performed conventional superconduction quantum interference device magnetometer studies of our thin film samples at temperatures down to 4.2 K, but have found these to be inconclusive, being dominated by the diamagnetic response of the Si substrate on which the films are grown. To probe the possible magnetic origins of the hysteresis reported here, we believe it is therefore necessary to perform direct, microscopic measurements of nanostructure magnetization at temperatures below 4.2 K. Unfortunately, we have no such experimental capability at present.

Since scattering at the interface between the Si substrate and silicide and the silicide and its surface oxide should be important in these crystalline samples, a large MR might be expected on applying a magnetic field *within* the plane of the NWs or films. In our experiments, however, the field is applied *normal* to this plane, and it is doubtful anyway that such a mechanism would yield the large hysteretic MR and the extreme sensitivity to temperature that we observe. While the time-dependent change of the resistance in Fig. 4 could possibly be attributed to electron trapping and/or detrapping by noninteracting paramagnetic centers, with a distribution of activation energies, we believe that the idea of interacting (albeit weakly) moments is required to explain all aspects of our data. The influence on transport of dilute paramagnetic impurities has been well studied for mesoscopic systems and does *not* give rise to hysteresis in the MR.<sup>15,34</sup> Rather, such centers result in increased dephasing of electrons and so suppress the WL/WAL MR, instead of giving the large MR that we observe.

### B. Some speculations on the possible origins of the hysteretic magnetoresistance

While the origins of the hysteretic MR that we observe remain to be conclusively determined, we believe that a plausible source is the presence of weakly interacting internal magnetic moments associated with unpaired electron spins on DBs. The importance of such DBs for determining the electrical properties of complementary-metal-oxide-semiconductor devices is well documented,<sup>35</sup> in which they arise naturally in high densities due to the presence of unterminated Si bonds at the Si/SiO<sub>2</sub> interface, with a density that depends strongly on the preparation conditions. Magnetic ordering of these local moments has been predicted theoretically for Si surfaces,<sup>5,6</sup> and evidence for this ordering has even been obtained experimentally.<sup>36,37</sup> (Indeed, there have even been reports of ferromagneticlike behavior in silicon in the presence of deliberately induced disorder<sup>38</sup>.) In the context of this work, there is a significant evidence to suggest that DBs may also exist near the surface of metallic silicides. Firstly, it is known<sup>39–42</sup> from studies of the epitaxial growth of both NiSi<sub>2</sub> and TiSi<sub>2</sub> that their surfaces do *not* consist of pure silicide. Rather, in spite of their different reaction mechanisms due to inter-diffusion during, and air exposure after, silicidation, they consist (from the top down) of a cap layer of SiO<sub>2</sub> (and nonstoichiometric SiO<sub>x</sub>), Si-rich, and metal-rich regions, and finally, stoichiometric silicide. In transmission-electron-microscopy studies,<sup>25</sup> we consistently

observe the presence of a 20–40 Å amorphous layer on the top surface of our silicide NWs that appears to indicate the presence of these nonstoichiometric regions. The presence of the nonstoichiometric SiO<sub>x</sub> and Si-rich regions could be an obvious source of DBs. Secondly, it has been suggested that steps at the surface of the silicide can act as a source of non-stoichiometric point defects.<sup>22</sup> Thirdly, we note that there have been reports of magnetic behavior in studies of TiSi<sub>x</sub> and VSi<sub>x</sub> films close to the metal-insulator transition.<sup>7</sup> In this work, it was demonstrated that the Ti and V *3d* states carry no magnetic moment in these amorphous alloys, and the observed magnetic character was ascribed instead to DBs generated by the amorphous Si. The effects of this magnetization were found to be particularly pronounced at low temperatures, below 10 K. Such a mechanism could certainly be relevant to the Ti and Ni silicide systems that we study and, being restricted to the silicide interface, should become increasingly important on going from thick to thin films and, ultimately, to NWs, just as we observe.

While the presence of local moments is one requirement for the observation of magnetic behavior, an *interaction* among these moments is also required. With regards to this latter issue, an important feature of the hysteretic MR that we observe is its quenching with increase of temperature to of order a few kelvins. Since we do not measure magnetic properties directly in our experiments, but rather infer information on them from the results of electrical measurements, some care is needed in interpreting this result. We believe, in particular, that the suppression of the hysteretic MR at higher temperatures is due to an associated quenching of the *interaction* among the DBs (and *not* the disappearance of the DBs themselves). To clarify this, we point out that, while the quantum MR in our NWs is only eventually suppressed with increase of temperature to ~30 K,<sup>25</sup> the hysteresis washes out well before this. We can therefore infer that the suppression of the hysteresis does not arise from our inability to detect it as the MR vanishes. Instead, the indication is that the hysteresis is truly a low-temperature phenomenon that is characterized by the presence of a weak interaction (with a characteristic energy scale of the order of meV) among the local moments. This conclusion is consistent with our studies of the dynamic properties of the MR hysteresis (Fig. 4), which were found to be characterized by a stretched exponential with a stretch parameter ( $\beta$ ) close to 1. As was noted already, such large values of  $\beta$  are indicative of a weak interaction among the moments.

It is our belief that an important clue as to the origin of the interaction among the DBs is provided by the very large magnitude, of the order of 100%, of the MR that we observe (Fig. 1). In typical disordered metals, the MR is at most on the order of a few percent and is proportional to the phase-coherence length, which decreases in the presence of magnetic scattering centers.<sup>43</sup> This comparison therefore leads us to suggest that the hysteretic MR arises from a phenomenon in which the conduction electrons in the silicide mediate the coupling among the (otherwise) weakly interacting surface magnetic moments. For this Ruderman-Kittel-Kasuya-Yosida (RKKY)-type mechanism to be effective, one would require the coherent propagation of electron spins between the DBs. As noted earlier, however, these materials exhibit strong

spin-orbit scattering, which should tend to suppress such a coupling mechanism. This scattering occurs on a time scale  $\tau_{so}$ , from which we can define a characteristic temperature scale  $T_{so} \sim \hbar / k_B \tau_{so}$ . Given a typical value of  $\tau_{so}$  for these materials of the order of 1 ps,<sup>22,25,43</sup> we obtain  $T_{so} \sim 7$  K. It is interesting that this crossover temperature is close to that at which the hysteresis disappears in our experiment. At this stage, we therefore suggest that the quenching of the hysteresis arises from a disruption of coupling between the DBs, as electron phase coherence becomes suppressed above a few kelvins.

## VI. CONCLUSIONS

In conclusion, we have demonstrated a large (as much as 100%) and strongly hysteretic MR in nominally nonferromagnetic silicide films and NWs. This unusual MR is quenched above a few kelvins, where conventional behavior due to WAL is recovered. The dynamic characteristics of this

effect are suggestive of the weak interaction of localized paramagnetic moments, and we have suggested that the source of these moments may be DBs that form in the non-stoichiometric surface layers of the silicides. A remarkable feature of the hysteretic MR is its extremely large magnitude, which clearly cannot be accounted for by the concept of perturbative conductance corrections that underpins WL theory. While we do not have a full explanation at present, our observations point to a transport mechanism, in which the conduction electrons are strongly coupled to weakly interacting surface magnetic moments. The suggestion of our results is that the interaction among the local moments is mediated by the conduction electrons themselves, giving rise to a new form of quantum magnetoresistance.

## ACKNOWLEDGMENTS

This work was supported by the National Science Foundation (ECS-0224163).

- 
- <sup>1</sup>A. Vilan, A. Shanzer, and D. Cahen, *Nature (London)* **404**, 166 (2000).
- <sup>2</sup>Y. Cui, Q. Wei, H. Park, and C. M. Lieber, *Science* **293**, 1289 (2001).
- <sup>3</sup>D. M. Gillingham, C. Müller, and J. A. C. Bland, *J. Phys.: Condens. Matter* **15**, L291 (2003).
- <sup>4</sup>D. M. Gillingham, C. Müller, J. Hong, R. Q. Wu, and J. A. C. Bland, *J. Phys.: Condens. Matter* **18**, 9135 (2006).
- <sup>5</sup>C. F. Bird and D. R. Bowler, *Surf. Sci.* **531**, L351 (2003).
- <sup>6</sup>E. F. Sheka, E. A. Nikitina, and V. A. Zayets, *Surf. Sci.* **532–535**, 754 (2003).
- <sup>7</sup>A. Yu. Rogatchev and U. Mizutani, *J. Phys.: Condens. Matter* **12**, 4837 (2000).
- <sup>8</sup>P. Crespo, R. Litrán, T. C. Rojas, M. Multigner, J. M. de la Fuente, J. C. Sánchez-López, M. A. García, A. Hernando, S. Penadés, and A. Fernández, *Phys. Rev. Lett.* **93**, 087204 (2004).
- <sup>9</sup>I. Carmeli, G. Leituss, R. Naaman, S. Reich, and Z. Vager, *J. Chem. Phys.* **118**, 10372 (2003).
- <sup>10</sup>Z. Vager and R. Naaman, *Phys. Rev. Lett.* **92**, 087205 (2004).
- <sup>11</sup>A. Hernando, P. Crespo, and M. A. Garcia, *Phys. Rev. Lett.* **96**, 057206 (2006).
- <sup>12</sup>A. Hernando, P. Crespo, M. A. Garcia, E. Fernandez-Pinel, J. de la Venta, A. Fernandez, and S. Penades, *Phys. Rev. B* **74**, 052403 (2006).
- <sup>13</sup>P. Crespo, M. A. Garcia, E. Fernandez-Pinel, M. Multigner, D. Alcantara, J. M. de la Fuente, S. Penades, and A. Hernando, *Phys. Rev. Lett.* **97**, 177203 (2006).
- <sup>14</sup>E. Guerrero, T. C. Rojas, M. Multigner, P. Crespo, M. A. Munoz-Marquez, M. A. Garcia, A. Fernandez, and A. Hernando, *Acta Mater.* **55**, 1723 (2007).
- <sup>15</sup>G. Bergmann, *Phys. Rep.* **107**, 1 (1984).
- <sup>16</sup>C. Sangregorio, T. Ohm, C. Paulsen, R. Sessoli, and D. Gatteschi, *Phys. Rev. Lett.* **78**, 4645 (1991).
- <sup>17</sup>W. Wernsdorfer, R. Sessoli, A. Caneschi, D. Gatteschi, A. Cornia, and D. Maillly, *J. Appl. Phys.* **87**, 5481 (2000).
- <sup>18</sup>I. Chiorescu, W. Wernsdorfer, A. Müller, H. Bögge, and B. Barbara, *Phys. Rev. Lett.* **84**, 3454 (2000).
- <sup>19</sup>F. Nava, K. N. Tu, E. Mazzega, M. Michelini, and G. Queirolo, *J. Appl. Phys.* **61**, 1085 (1987).
- <sup>20</sup>S. P. Murarka, *Silicides For VLSI Applications* (Academic, New York, 1983).
- <sup>21</sup>S. Liang, R. Islam, D. J. Smith, P. A. Bennett, J. R. O'Brien, and B. Taylor, *Appl. Phys. Lett.* **88**, 113111 (2006).
- <sup>22</sup>F. Jentzsch, R. Schad, S. Heun, and M. Henzler, *Phys. Rev. B* **44**, 8984 (1991).
- <sup>23</sup>D. Lenssen and S. Mantl, *Appl. Phys. Lett.* **71**, 3540 (1997).
- <sup>24</sup>H. Okino, I. Matsuda, R. Hobara, Y. Hosomura, S. Hasegawa, and P. A. Bennett, *Appl. Phys. Lett.* **86**, 233108 (2005).
- <sup>25</sup>J.-F. Lin, J. P. Bird, Z. He, P. A. Bennett, and D. J. Smith, *Appl. Phys. Lett.* **85**, 281 (2004).
- <sup>26</sup>G. Bergmann, *Phys. Rev. B* **28**, 2914 (1983).
- <sup>27</sup>R. G. Aitken, T. D. Cheung, J. S. Kouvel, and H. Hurdequint, *J. Magn. Magn. Mater.* **30**, L1 (1982).
- <sup>28</sup>S. Senoussi, *Phys. Rev. Lett.* **51**, 2218 (1983).
- <sup>29</sup>S. Senoussi and Y. Öner, *J. Appl. Phys.* **55**, 1472 (1984).
- <sup>30</sup>R. V. Chamberlin, *Phys. Rev. Lett.* **83**, 5134 (1999).
- <sup>31</sup>R. V. Chamberlin, G. Mozurkewich, and R. Orbach, *Phys. Rev. Lett.* **52**, 867 (1984).
- <sup>32</sup>R. Böhmer, B. Schiener, J. Hemberger, and R. V. Chamberlin, *Z. Phys. B: Condens. Matter* **99**, 91 (1995).
- <sup>33</sup>For a review, see I. Zutic, J. Fabian, and S. Das Sarma, *Rev. Mod. Phys.* **76**, 323 (2004).
- <sup>34</sup>J. Vranken, C. Van Haesendonck, and Y. Bruynseraede, *Phys. Rev. B* **37**, 8502 (1988).
- <sup>35</sup>R. F. Pierret, *Semiconductor Device Fundamentals* (Addison-Wesley, Reading, MA, 1996).
- <sup>36</sup>T. Suzuki, V. Venkataraman, and M. Aono, *Jpn. J. Appl. Phys., Part 2* **40**, L1119 (2001).
- <sup>37</sup>Z. Wu, T. Nakayama, M. Sakurai, and M. Aono, *Surf. Sci.* **386**, 311 (1997).
- <sup>38</sup>See T. Dubroca, J. Hack, and R. E. Hummel, *Appl. Phys. Lett.*

- 88**, 182504 (2006), and references therein.
- <sup>39</sup>S. Saitoh, H. Ishiwara, and S. Furukawa, Appl. Phys. Lett. **37**, 203 (1980).
- <sup>40</sup>J. C. Bean and J. M. Poate, Appl. Phys. Lett. **37**, 643 (1980).
- <sup>41</sup>S. A. Chambers, S. B. Anderson, H. W. Chen, and J. H. Weaver, Phys. Rev. B **34**, 913 (1986).
- <sup>42</sup>V. Hinkel, L. Sorba, H. Haak, and K. Horn, Appl. Phys. Lett. **50**, 1257 (1987).
- <sup>43</sup>J. J. Lin and J. P. Bird, J. Phys.: Condens. Matter **14**, R501 (2002).